ELSEVIER

Atmospheric Research 82 (2006) 489–502

ATMOSPHERIC RESEARCH

www.elsevier.com/locate/atmos

Comparison of Monte Carlo simulation methods for the calculation of the nucleation barrier of argon

Antti Lauri *, Joonas Merikanto, Evgeni Zapadinsky, Hanna Vehkamäki

University of Helsinki, Department of Physical Sciences, P.O. Box 64, FI-00014 University of Helsinki, Finland

Accepted 1 February 2006

Abstract

We compare two molecular Monte Carlo simulation methods, the discrete summation method and the growth/decay method, which calculate the vapor-liquid nucleation free energy barrier by simulating isolated clusters of fixed size without the surrounding vapor. The methods are applied to calculations of nucleation barriers of Lennard–Jones argon at 60 K and 80 K. Both of these methods are computationally efficient, as only isolated clusters without the surrounding vapor are simulated, and the methods can be applied with any given cluster definition. They give equivalent results to other methods where the vapor phase is also included. The discrete summation method is based on the calculation of the difference in free energies between two systems containing an n-cluster and an $(n-1)$-cluster plus one non-interacting (free) molecule. We show that the configurational space is not equivalent in the two systems. Hence, there has to be an additional term in the free energy calculation that accounts for several kT in magnitude. In contrast to previous studies we also show that it is not correct to prevent the overlap of the non-interacting molecule and another molecule by a zero or an arbitrarily small repulsive potential, but with a small excluded space around the free molecule.

Keywords: Nucleation; Monte Carlo simulation; Argon

1. Introduction

In the atmospheric research the nucleation of supersaturated vapor is a major point of interest (Kulmala, 2003). The main quantity obtained from the nucleation experiments and field measurements is the nucleation rate. From the theoretical point of view nucleation is dominated by energetics – the free energy barrier. Molecular simulations are able to describe the energetics of the nucleation phenomena most accurately out of all approaches. There are two main difficulties in molecular simulations to overcome, however. Pair potential models are currently incapable of correctly expressing the interactions between more complex molecules such as water, sulphuric acid or ammonia. Even ab initio calculations of small molecular clusters do not yet give satisfactory data to be compared with the experiments (Vehkamäki et al., 2004). Another difficulty lies in the selection of the most appropriate simulation method. There are a great number of molecular methods available, each having their own characteristics like accuracy, speed and suitability for different kinds of calculations. The aim of our study is to propose suitable, fast and accurate simulation methods for the nucleation free energy barrier calculations.

It is well known that the classical nucleation theory (Volmer and Weber, 1925; Becker and Döring, 1935; Zeldovich, 1942), even with its extensions (Lothe and

* Corresponding author. Tel.: +358 9 191 50716; fax: +358 9 191 50860.

E-mail address: antti.lauri@helsinki.fi (A. Lauri).

0169-8095/$ - see front matter © 2006 Elsevier B.V. All rights reserved.
doi:10.1016/j.atmosres.2006.02.006

Pound, 1962; Oxtoby and Evans, 1988; Dillmann and Meier, 1991), is not capable of giving a complete description of the nucleation processes. This is why molecular level approaches, like the Monte Carlo (MC) and molecular dynamic simulations, have recently gained more attention in the study of nucleation. Although the power of the simulation methods is still limited by computational constraints and the lack of reliable force fields in the study of atmospheric nucleation processes, the complexity of the systems that can be studied with these methods has increased dramatically in the last years. This makes the molecular approach to nucleation promising. Especially Monte Carlo simulations allow one to calculate the nucleation rate straightforwardly even for low saturation ratios. However, only few MC simulation results appear to be suitable for a comparison with the experiments. The controversial experimental results for nucleation of argon have not allowed one to make a conclusion on the compatibility between the molecular theory and the experimental data. In some cases the molecular theory gives results closer to experiment than the CNT, while in other cases the classical theory is more successful (Zahoransky et al., 1999; Wu et al., 1978; Pierce et al., 1971; Lewis and Williams, 1974; Matthew and Steinwandel, 1983; Steinwandel and Buchholz, 1984; Stein, 1974; Hoare et al., 1980; Garcia and Soler Torroja, 1981; ten Wolde and Frenkel, 1998; ten Wolde et al., 1999; Oh and Zeng, 1999; Hale, 1996). Comparison of the theory and experiment for homogeneous water nucleation gives more data for analysis. Neither the CNT nor MC simulations based on the statistical mechanics approach agree well with the absolute values of the experimental nucleation rate, but the MC simulations reproduce the experimental saturation ratio and temperature dependence, while the CNT is not able to predict the correct temperature dependence (Wölk and Strey, 2001; Merikanto et al., 2004). This is encouraging for the future development and improvement of the molecular approach to nucleation problems.

There are nowadays several different types of Monte Carlo simulation methods that have been developed for the study of nucleation. The common nominator for all these methods is the same: they all attempt to calculate the free energy barrier that separates the two phases. The height of the energy barrier is the key quantity that defines the rate of the process, the nucleation rate. The methods can be divided in two types. The first one is direct simulation of vapor to observe clustering (ten Wolde and Frenkel, 1998; Oh and Zeng, 1999; Chen et al., 2001). The second type is the simulation of isolated cluster to calculate the cluster free energy (Lee et al., 1973; Hale and Ward, 1982; Kusaka et al., 1998; Merikanto et al., 2004). At the first sight the direct simulation seems to be more rigorous than the simulation of isolated cluster. However, all reported methods of the first type assume the validity of the law of mass action (Abraham, 1974; Bijl, 1938; Band, 1939a,b; Frenkel, 1939b,a). From statistical mechanics we know that if an equilibrium cluster distribution exists, then the cluster concentration can be calculated through the cluster partition function. Then, the only more general feature of direct vapor simulation is taking the cluster–monomer and cluster–cluster interaction into account. As was shown by Oh and Zeng (2000) their contributions are negligibly small for low densities and for high densities they can be taken into account through the mean field approach. This gives us the equivalence of two types of vapor simulations. Simulations of the isolated cluster using the discrete summation method (Hale and Ward, 1982) and the growth/decay MC approach (Merikanto et al., 2004) have two advantages. First, they are much less time consuming than simulations of the entire vapor–cluster system since they do not need very large number of molecules in the simulating system. Second, these two methods do not require simulations at different saturation ratios: one simulation yields nucleation barrier for all saturation ratios at one temperature. In the present study we have concentrated on the theoretical background of the discrete summation method (Hale and Ward, 1982) and its comparison to the growth/decay MC approach (Merikanto et al., 2004).

2. The discrete summation method

A starting point for the reversible work of formation of clusters of size n is the law of mass action (Abraham, 1974; Bijl, 1938; Band, 1939a,b; Frenkel, 1939a,b)

$$\frac{\mathcal{N}_n}{Z(n)} = \left(\frac{\mathcal{N}_1}{Z(1)}\right)^n, \tag{1}$$

where $\mathcal{N}_n$ is the number of clusters of size n in the vapor, and $Z(n)$ is the canonical partition function

$$Z(n) = \frac{\Lambda^{-3n} q(n)}{n!}, \tag{2}$$

where $\Lambda=(h/2\pi mkT)^{1/2}$ is the de Broglie wavelength, where h is the Planck constant, m is the mass of a molecule, k is the Boltzmann constant, and T is the

temperature. Furthermore, $q(n)$ is the configurational integral

$$q(n) = \int_{\text{cluster}} \cdots \int \exp\left(-\frac{U_n(\boldsymbol{R}_1, \ldots, \boldsymbol{R}_i, \ldots, \boldsymbol{R}_n)}{kT}\right) \times \mathrm{d}\boldsymbol{R}_1 \ \ldots \ \mathrm{d}\boldsymbol{R}_n, \tag{3}$$

where $\boldsymbol{R}_i$ is the position vector of the ith molecule, and U_n is the potential energy of the cluster.

The law of mass action [Eq. (1)] can be rewritten as

$$\mathcal{N}_n = \mathcal{N}_1 \exp\left(-\frac{\Delta W}{kT}\right), \tag{4}$$

where

$$\Delta W = -kT\left[\ln\left(\frac{q(n)}{n!}\right) - n\ln q(1) - (n-1)\ln\mathcal{N}_1\right] \tag{5}$$

is often referred to as the reversible work of formation of an n-cluster (see e.g. Reiss and Bowles, 1999). Using the procedure of Hale and Ward (Hale and Ward, 1982; Hale, 1996), Eq. (5) can be transformed to a more convenient form for the purpose of molecular simulations.

We make advantage of the fact that the configurational integral of an n-cluster can be obtained by multiplying $[q(i)]/[q(i-1)]$ over all the cluster sizes smaller than n:

$$q(n) = \frac{q(n)}{q(n-1)} \times \frac{q(n-1)}{q(n-2)} \times \cdots \times \frac{q(2)}{q(1)} \times q(1). \tag{6}$$

The logarithm of this product can further be transformed to the form

$$\ln q(n) = \sum_{i=2}^{n} \ln\left(\frac{q(i)}{q(i-1)}\right) + \ln q(1). \tag{7}$$

Knowing that $q(1)=V$, where V is the volume of the system, the work of formation can be calculated by

$$\Delta W = kT \sum_{i=2}^{n} \left[-\ln\frac{q(i)}{q(i-1)V} + \ln i - \ln\mathcal{N}_1\right]. \tag{8}$$

Further on, we treat the denominator $q(i-1)V$ in the logarithm inside the summation in Eq. (8) differently from the way of Hale and Ward. This difference will produce a distinction in the partition function of the cluster.

After the transformation from the laboratory coordinates $\boldsymbol{R}$ to the center of mass coordinates $\boldsymbol{R}'$ the expression of the configurational integral for the clusters of n molecules becomes

$$q(n) = n^3 q_{\mathrm{cm}(n)}(n) V, \tag{9}$$

where

$$q_{\mathrm{cm}(n)}(n) = \int_{n-\text{cluster}} \cdots \int \exp\left(-\frac{U_n(\boldsymbol{R}'_1, \ldots, \boldsymbol{R}'_{n-1})}{kT}\right) \times \mathrm{d}\boldsymbol{R}'_1 \ \ldots \ \mathrm{d}\boldsymbol{R}'_{n-1}, \tag{10}$$

and n^3 is the Jacobian determinant of the coordinate transformation, and

$$\int \mathrm{d}\boldsymbol{R}_{\mathrm{cm}} = V. \tag{11}$$

Similarly in the center of mass coordinates $\boldsymbol{R}''$ for an $(n-1)$-cluster

$$q(n-1) = (n-1)^3 q_{\mathrm{cm}(n-1)}(n-1) V, \tag{12}$$

where

$$q_{\mathrm{cm}(n-1)}(n-1) = \int_{n-1-\text{cluster}} \cdots \int \times \exp\left(-\frac{U_{n-1}(\boldsymbol{R}''_1, \ldots, \boldsymbol{R}''_{n-2})}{kT}\right) \mathrm{d}\boldsymbol{R}''_1 \ \ldots \ \mathrm{d}\boldsymbol{R}''_{n-2}, \tag{13}$$

and

$$\int \mathrm{d}\boldsymbol{R}'_{\mathrm{cm}} = V. \tag{14}$$

Let us consider two systems, A and B. System A consists of n molecules in a cluster. The center of mass of system A is fixed. System B is otherwise exactly the same as system A, but there is one free molecule, which does not interact with the other molecules in the cluster. Clearly

$$q_{\mathrm{A}}(n) = q_{\mathrm{cm}(n)}(n). \tag{15}$$

To get the relation between $q_{\mathrm{B}}(n)$, which is obtained from our simulation, and $q_{\mathrm{cm}}(n-1)$, which is needed in Eq. (8), we need to consider the configurational integral in more detail. Deciding that the nth molecule in the n-cluster is always the one not interacting with the other molecules we can write the configurational integral for system B in the center of mass coordinates of the n-cluster simply as

$$q_{\mathrm{B}}(n) = \int_{n-\text{cluster}} \cdots \int \exp\left(-\frac{U_n(\boldsymbol{R}'_1, \ldots, \boldsymbol{R}'_{n-1})}{kT}\right) \mathrm{d}\boldsymbol{R}'_1 \ \ldots \ \mathrm{d}\boldsymbol{R}'_{n-1}, \tag{16}$$

where $\boldsymbol{R}'_i$ is the coordinate of molecule i in the center of mass coordinates of the n-cluster. After the transformation

to the center of mass coordinates of a system of $n-1$ interacting molecules ($\boldsymbol{R}''$) the configurational integral becomes

$$q_{\mathrm{B}}(n) = \int_{n-\mathrm{cluster}} \cdots \int \exp\left(-\frac{U_n(\boldsymbol{R}''_1, \ldots, \boldsymbol{R}''_{n-2})}{kT}\right) \times \mathrm{d}\boldsymbol{R}''_1 \ \ldots \ \mathrm{d}\boldsymbol{R}''_{n-2}\mathrm{d}\boldsymbol{R}'_{\mathrm{cm}}(n-1)^3. \quad (17)$$

The center of mass position is fixed. However, in system B the center of mass position includes also the coordinates of the non-interacting molecule. Thus, integration over the center of mass of the $(n-1)$-cluster reflects the movement of the center of mass in system B.

Instead of integrating over the center of mass coordinate of the $(n-1)$-cluster $\boldsymbol{R}'_{\mathrm{cm}}$ we can integrate over the non-interacting molecule, since

$$\boldsymbol{R}''_n = -n\boldsymbol{R}'_{\mathrm{cm}} \Rightarrow \mathrm{d}\boldsymbol{R}'_{\mathrm{cm}} = \frac{\mathrm{d}\boldsymbol{R}''_{\mathrm{n}}}{n^3}, \quad (18)$$

where $1/n^3$ is again the Jacobian determinant of the transformation. This coordinate transformation is illustrated in Fig. 1. The transformation then leads to

$$q_{\mathrm{B}}(n) = \int_{n-\mathrm{cluster}} \cdots \int \exp\left(-\frac{U_n(\boldsymbol{R}''_1, \ldots, \boldsymbol{R}''_{n-2})}{kT}\right) \times \mathrm{d}\boldsymbol{R}''_1 \ \ldots \ \mathrm{d}\boldsymbol{R}''_{n-2}\mathrm{d}\boldsymbol{R}''_{\mathrm{n}} \frac{(n-1)^3}{n^3}. \quad (19)$$

Now we have to consider the boundary conditions of the cluster definition. Whereas the cluster of n molecules follows the cluster definition, the cluster of $n-1$ interacting molecules and one non-interacting molecule does not necessarily fulfill the conditions required by the cluster definition for the $(n-1)$-cluster. To overcome this we will formally split the configurational integral into two parts:

$$q_{\mathrm{B}}(n) = \int_{(n-1)-\mathrm{cluster}} \cdots \int \exp\left(-\frac{U_n(\boldsymbol{R}''_1, \ldots, \boldsymbol{R}''_{n-2})}{kT}\right) \mathrm{d}\boldsymbol{R}''_1 \ \ldots \ \mathrm{d}\boldsymbol{R}''_{n-2}\mathrm{d}\boldsymbol{R}''_{\mathrm{n}} \frac{(n-1)^3}{n^3} + \int_{\substack{n-\mathrm{cluster} \\ \mathrm{not}(n-1)-\mathrm{cluster}}} \cdots \int \exp\left(-\frac{U_n(\boldsymbol{R}''_1, \ldots, \boldsymbol{R}''_{n-2})}{kT}\right) \mathrm{d}\boldsymbol{R}''_1 \ \ldots \ \mathrm{d}\boldsymbol{R}''_{n-2}\mathrm{d}\boldsymbol{R}''_{\mathrm{n}} \frac{(n-1)^3}{n^3}. \quad (20)$$

The first integral in "Eq. (20) includes only those configurations of the cluster where $n-1$ interacting molecules form an $(n-1)$-cluster and together with the free molecule form an n-cluster. The second integral includes only configurations where n molecules belong to the same cluster, but $n-1$ interacting molecules can not be considered as an $(n-1)$-cluster.

Furthermore, integration over the position of the nth molecule gives the volume available for the free molecule. Now we will mark the sum of the two integrals in Eq. (20) as

$$q_{\mathrm{B}}(n) = (I_1 + I_2)\frac{(n-1)^3}{n^3} = I_1[1+\delta(n)]\frac{(n-1)^3}{n^3}, \quad (21)$$

where $\delta(n)$ accounts for the configurations in system B, which do not fulfill the conditions required by the cluster definition for the $(n-1)$-cluster.

Multiplying the right hand side of Eq. (20) by $[q_{\mathrm{cm}}(n-1)]/[q_{\mathrm{cm}}(n-1)]$ and knowing that $I_1 = \langle v_{\mathrm{free}}\rangle q_{\mathrm{cm}}(n-1)$, where $\langle v_{\mathrm{free}}\rangle$ is the canonically averaged volume available for the free molecule, when it forms an n-cluster together with an cluster of $n-1$ interacting molecules, we will end up at

$$q_{\mathrm{B}} = \frac{\langle v_{\mathrm{free}}\rangle q_{\mathrm{cm}}(n-1)(n-1)^3}{n^3}[1+\delta(n)]. \quad (22)$$

Using Eqs. (15) and (22) the ratio between the configurational integrals of clusters of sizes n and $n-1$ is

$$\frac{q_{\mathrm{cm}}(n)}{q_{\mathrm{cm}}(n-1)} = \frac{q_{\mathrm{A}}\langle v_{\mathrm{free}}\rangle(n-1)^3[1+\delta(n)]}{q_{\mathrm{B}}n^3}. \quad (23)$$

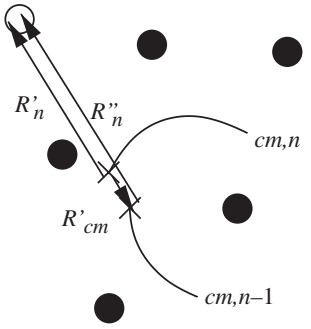

Fig. 1. A schematic picture of the coordinate transformation from the center of mass coordinates of the n-cluster to the center of mass coordinates of the $(n-1)$-cluster. The interacting molecules are shown as filled circles, and the nth molecule (not interacting) as an open circle. The crosses correspond to the center of mass positions of the n- and $(n-1)$-clusters. The position vector of the non-interacting molecule is denoted by $\boldsymbol{R}'_n$ in the n-cluster center of mass coordinates, and by $\boldsymbol{R}''_n$ in the $(n-1)$-cluster center of mass coordinates. The relation between the center of mass coordinate of the $(n-1)$-cluster and the coordinate of the non-interacting molecule in the center of mass coordinates of the n-cluster is obvious.

Using the conventional relation between the Helmholtz free energy $F(n)$ and the configurational integral,

$$F(n) = -kT\ln q(n), \tag{24}$$

and inserting Eqs. (9), (12), and (23) into Eq. (8) we will end in the expression for the reversible work of formation of an n-cluster

$$\Delta W = \sum_{i=2}^{n} \left(F_A - F_B - kT\ln[1+\delta(i)] + kT\ln\frac{i}{\rho_{sv}\langle v_{free}\rangle} - kT\ln S \right), \tag{25}$$

where we have used the relation of the monomer density to that in the saturated vapor (ρ_{sv})

$$\frac{\mathcal{N}_1}{V} = \rho_{sv} S \tag{26}$$

and saturation ratio S.

Eq. (25) contains three unknown values, namely the Helmholtz free energy difference between systems A and B, $F_A - F_B$, the δ-term $\ln(1+\delta)$, and v_{free}. All these values can be simulated by means of MC simulations. The details of the methods are presented in the following section. The way of calculating of the volume v_{free} depends on the cluster definition. For the cluster definition of Lee, Barker and Abraham (LBA) (Lee et al., 1973) the available volume v_{free} is clearly the volume of an n-cluster. For the other widely used cluster definition, introduced by Stillinger (1963), the interpretation of this volume is not so obvious. The cluster definition also affects the choice of the simulation volume. For the LBA cluster it is simply the volume of the n-cluster, while for the Stillinger cluster the simulation volume is formally the volume of the system, V. In practice, the simulation volume for the Stillinger cluster can be chosen to be big enough to include all possible configurations of the cluster with its fixed center of mass. The effectively searched volume is confined by the Boltzmann factor and the cluster definition, and it is clearly different for systems A and B: due to the free monomer, the cluster in the latter system can produce looser configurations than in the former one. However, for the method presented in the following section it is only important that effective volumes of the simulated systems demonstrate good overlapping, which is certainly the case.

In their formulation Hale and Ward did not use the concept of the reversible work of formation. However, if we apply their formalism for the calculation of the work of formation, we find that our results differ from the results of Hale and Ward by the term resulting from the second integral in Eq. (20). Thus, the total difference is

$$\text{difference} = -kT\sum_{i=2}^{n}\ln[1+\delta(i)]. \tag{27}$$

3. The overlapping distribution method

We employed the overlapping distribution method (Bennett, 1976) along with the discrete summation method described in the previous section to obtain the free energy difference between two closely related systems. In our case, these two cases are the systems A and B described in Section 2. We simulated both systems separately in the canonical ensemble. While simulating system A we accumulated a probability distribution $\mathcal{P}_A(\Delta U)$, where $\Delta U = U_A - U_B$ is the total potential energy difference between systems A and B. Similarly, we produced a probability distribution $\mathcal{P}_B(\Delta U)$ during the simulation of system B. Wherever the histograms overlap, the Helmholtz free energy difference between the systems is obtained by

$$\Delta F = \Delta U + kT\ln\left(\frac{\mathcal{P}_A(\Delta U)}{\mathcal{P}_B(\Delta U)}\right), \tag{28}$$

where $\Delta F = F_A - F_B$ corresponds to the free energy difference between the systems.

We used the cluster definition of Stillinger (1963). When using this definition, the boundary condition discussed in context of the second integral in Eq. (20) is constituted of such exceptional configurations where the non-interacting molecule in an n-cluster forms the only link between two parts of the cluster and the exclusion of the non-interacting molecule would break the $(n-1)$-cluster. These exceptional configurations give rise for the δ-term. The Bennett method can be used for calculation of the δ-term as well. When simulating system B the exceptional configurations are not forbidden. Suppose, there is a system C, which is exactly the same as the system B but the exceptional configurations are forbidden or equally have very high positive energy. Applying an "imaginary overlapping distribution method" shown in Fig. 2 we are able to formulate the additional term. The ratio between the configurational integrals of the two systems (i.e. their free energy difference) is then obtained as the ratio $\mathcal{P}_C/\mathcal{P}_B$ at the only overlapping point ($\Delta U \equiv U_C - U_B = 0$). By means of the term $1+\delta(n)$ in Eq. (21) this difference is now given by

$$1+\delta(n) = \frac{N(n)}{N(n) - N_e(n)}, \tag{29}$$

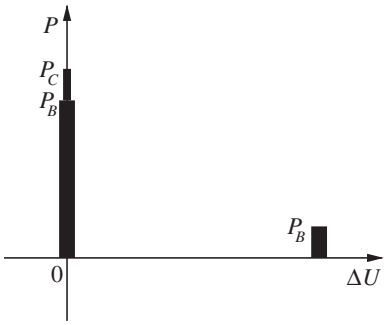

Fig. 2. The idea behind the "imaginary Bennett method" used to determine the term $1+\delta(n)$. The only point, where the probability distributions overlap, is at $\Delta U=0$.

where $N(n)$ is the total number of sampled configurations of an n-cluster, and $N_e(n)$ is the number of exceptional configurations, in which the non-interacting molecule is the only link between two parts of the cluster. In practice, N_e is calculated when simulating system B. Thus, there is no need to simulate system C.

For the simulations we define a factor λ, which is used to turn the interaction between two molecules on and off. The value of λ can vary between 0 and 1, corresponding to zero and full interaction. In terms of our formalism given in Section 2, the value $\lambda=1$ corresponds to system A, whereas $\lambda=0$ corresponds to system B.

Particularly when simulating an ensemble where there is no interaction with one of the molecules and the rest of the cluster, unrealistically high potential energy differences between systems A and B arise due to the free molecule getting very near a cluster molecule. These situations disturb the probability distributions. In order to prevent the disturbance λ can be set close to, but not equal to zero in the non-interacting case to prevent molecule overlapping. In this case, however, we allow more configurational space for the free molecule. This will lead to a systematic error in the results. Another way of preventing the molecule overlap is to restrict the nearest allowed distance between the non-interacting molecule and the cluster molecules to a certain value.

In our simulations we have estimated a numerical value for the canonically averaged volume $\langle v_{\text{free}}\rangle$ available for the free molecule. In practice this was done by a set of brute force Monte Carlo runs during the simulations. For each randomly chosen configuration we placed a sphere centered in the center of mass position of the $(n-1)$-cluster. The radius of the sphere was the critical distance of the cluster definition added to the distance between the center of mass and the molecule furthest away from the center of mass. Evenly distributed random points inside this sphere were selected for the configuration during the simulation of ensemble A, and the number of points belonging to the cluster according to the cluster definition was counted. Then the available volume was obtained by multiplying the volume of the sphere and the fraction of the points belonging to the cluster. Averaging was done over two thousand configurations.

4. The growth/decay Monte Carlo method

In the growth/decay Monte Carlo method we simulate one cluster at a time with a fixed number of particles. The cluster configuration space is traced out in a canonical Metropolis simulation. Instead of letting the cluster size fluctuate in a grand canonical fashion, we only calculate the probabilities for the grand canonical annihilation and creation moves. We have shown how these probabilities can be linked to the kinetic condensation and evaporation coefficients of Becker and Döring (1935). The full derivation can be found elsewhere (Merikanto et al., 2004; Vehkamäki and Ford, 2000).

We consider n fully interacting cluster particles with $n_{\max}-n$ non-interacting particles at arbitrary positions inside a large simulation box of volume V, the center of mass of the cluster being placed at the center of the simulation box. The annihilation probability $A(n, \{\mathbf{R}_i\}\ominus\mathbf{R}_j)$ for an interacting cluster particle at a position $\mathbf{R}_j$ from configuration $\{\mathbf{R}_i\}$ is given by

$$A(n,\{\mathbf{R}_i\}\ominus\mathbf{R}_j) = \frac{n}{\gamma VZ}\exp\left\{\frac{-[U_{n-1}(\{\mathbf{R}_i\}\ominus\mathbf{R}_j)-U_n(\{\mathbf{R}_i\})]}{kT}\right\}, \quad (30)$$

where $\gamma=1/\lambda^{-3}$, λ is the de Broglie wavelength of the particles, $U_n(\{\mathbf{R}_i\})$ is the total interaction energy associated with the configuration $\{\mathbf{R}_i\}$, k is the Boltzmann constant, and T is the temperature. The notation $\{\mathbf{R}_i\}\ominus\mathbf{R}_j$ indicates that the particle at position $\mathbf{R}_j$ is taken away from configuration $\{\mathbf{R}_i\}$. The activity $Z=\exp[\mu/(kT)]$, where μ is the chemical potential, is equal to the density of the surrounding vapor ρ under the ideal gas assumption. The probability to turn a non-interacting particle into a fully interacting particle, the creation probability $C(n, \{\mathbf{R}_i\}\oplus\mathbf{R}_k)$, is given by

$$C(n,\{\mathbf{R}_i\}\oplus\mathbf{R}_k) = \frac{\gamma VZ}{n+1}\exp\left\{\frac{-[U_{n+1}(\{\mathbf{R}_i\}\oplus\mathbf{R}_k)-U_n(\{\mathbf{R}_i\})]}{kT}\right\}. \quad (31)$$

The probability that an n-cluster decays into an $(n-1)$-cluster during a Monte Carlo step is given by summing

up the individual decay probabilities for each interacting cluster particle and normalizing the sum with the number of attempted annihilations n,

$$D_n(\{\mathbf{R}_i\}) = \frac{\alpha_D}{n}\sum_{j=1}^{n} \delta_{clu}\min[1,A(n,\{\mathbf{R}_i\}\ominus\mathbf{R}_j)], \quad (32)$$

where α_D is the probability that the annihilation is attempted during the given Monte Carlo step, and δ_{clu} is zero when annihilation would result in splitting the resulting $(n-1)$-cluster into two or more clusters according to given cluster definition, and 1 otherwise.

In a similar fashion, the probability that an n-cluster grows into an $(n+1)$-cluster during a Monte Carlo step is given by summing up the $n_{max}-n$ possible non-interactive particle creations into interactive particles and normalizing with the number of attempts $n_{max}-n$

$$G_n(\{\mathbf{R}_i\}) = \frac{\alpha_C}{n_{max}-n}\sum_{k=1}^{n_{max}-n} \delta_{clu}\min[1,C(n,\{\mathbf{R}_i\}\oplus\mathbf{R}_k)]. \quad (33)$$

The creation is attempted during a Monte Carlo step with a probability $\alpha_C=\alpha_D$. δ_{clu} now ensures that the created particle is a part of the resulting cluster according to the applied cluster definition. During a simulation, $D(n,\{\mathbf{R}_i\})$ and $G(n,\{\mathbf{R}_i\})$ are calculated for a large number of configurations $\{\mathbf{R}_i\}$ to gain the canonical ensemble averages of the growth and decay probabilities $\bar{G}_n$ and $\bar{D}_n$. This procedure is carried out for each cluster size n separately. Earlier (Merikanto et al., 2004), we have showed that the work of cluster formation of an n-cluster ΔW_n has a simple relation to $\bar{G}_n$ and $\bar{D}_n$ given by

$$\Delta W_n = -kT\sum_{j=2}^{n} \ln\frac{\bar{G}_{j-1}}{\bar{D}_j}. \quad (34)$$

In the kinetic approach ΔW_n is given by (Becker and Döring, 1935; Kashchiev, 2000)

$$\Delta W_n = -kT\sum_{j=2}^{n} \ln\frac{\beta_{j-1}}{\alpha_j}, \quad (35)$$

so there is a direct relation between the Becker and Döring kinetic evaporation and condensation constants β_j and α_j and grand canonical growth and decay probabilities $\bar{G}_n$ and $\bar{D}_n$

$$\frac{\bar{G}_{j-1}}{\bar{D}_j} = \frac{\beta_{j-1}}{\alpha_j}. \quad (36)$$

It is important to notice that the relation $\bar{G}_{j-1}/\bar{D}_j$ does not depend on the size of the simulation box. This can be seen by taking V sufficiently large. Then, the following inequalities always hold

$$A(n,\{\mathbf{R}_i\}\ominus\boldsymbol{R}_j) < 1 \quad (37)$$

$$C(n,\{\mathbf{R}_i\}\oplus\boldsymbol{R}_k) > 1, \quad (38)$$

and the minimum functions from Eqs. (32) and (33) can be removed, yielding

$$G_n(\{\mathbf{R}_i\}) = \frac{\alpha_C}{n_{max}-n}\sum_{k=1}^{n_{max}-n} \delta_{clu} = \frac{\alpha_C V_{C,n}}{V} \quad (39)$$

$$D_n(\{\mathbf{R}_i\}) = \frac{\alpha_D}{n}\sum_{j=1}^{n} \delta_{clu}A(n,\{\mathbf{R}_i\}\ominus\mathbf{R}_j)$$

$$= \frac{\alpha_D}{\gamma ZV}\sum_{j=1}^{n} \delta_{clu}\exp\left\{\frac{-[U_{n-1}(\{\mathbf{R}_i\}\ominus\mathbf{R}_j)-U_n(\{\mathbf{R}_i\})]}{kT}\right\} \quad (40)$$

where $V_{C,n}$ is the volume of the space where the creation is allowed.

From the above equations, it can also be seen that the activity Z containing the saturation ratio dependence appears only in the multiplier of the decay probability. Thus, the simulation results for $\bar{G}(j-1, Z_1)/\bar{D}(j, Z_1)$ gained by using activity Z_1 can be scaled to obtain results for another activity Z_2 as well. The scaling then reads as

$$\frac{\bar{G}(j-1,Z_2)}{\bar{D}(j,Z_2)} = \frac{Z_2}{Z_1}\frac{\bar{G}(j-1,Z_1)}{\bar{D}(j,Z_1)}. \quad (41)$$

Thus there is no need for separate simulations for different saturation ratios.

5. Overview of the methods and details of the simulations

The discrete summation and growth/decay methods both calculate the vapor–liquid nucleation free energy barrier by simulating single isolated clusters of fixed size without the surrounding vapor. Fig. 3 shows a simplified illustration of the two methods.

In the discrete summation method two nearly identical ensembles are simulated simultaneously. One of the systems contains n molecules (ensemble A) and the other one contains $n-1$ molecules plus one free non-interacting molecule (ensemble B). The molecules are moved inside the system according to the Metropolis algorithm so that the n-cluster's center

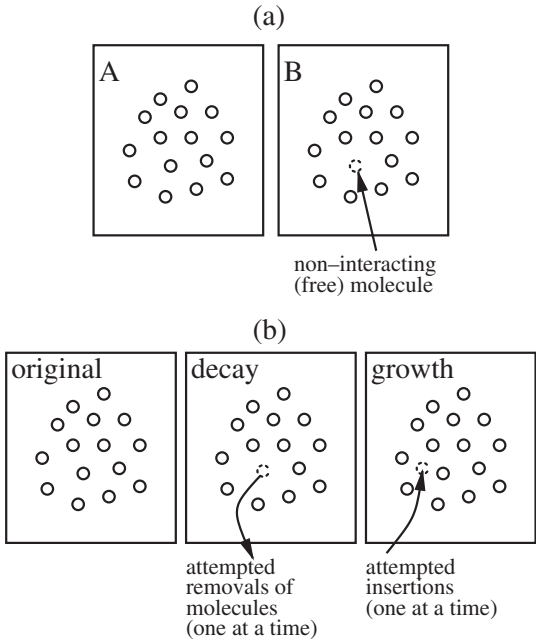

Fig. 3. A simplistic figure about the ideas behind (a) the overlapping distribution method and (b) the growth/decay method.

of mass is kept fixed. First the algorithm is applied to ensemble A, and the molecules in system B are moved accordingly. The potential energy difference between the two systems is recorded in a probability distribution (histogram). Then the algorithm is applied to ensemble B, and the molecules in system A are moved accordingly, producing a second probability distribution of the potential energy differences. The free energy is calculated from the overlap of the two histograms using Eq. (28).

In the growth/decay method we are simulating only one ensemble instead of two. We calculate the grand canonical decay and growth probabilities given by Eqs. (32) and (33) for n-molecule cluster configurations, which are created using the canonical Metropolis algorithm. The growth probability for a specific molecular configuration is calculated by inserting molecules at random positions around the cluster and calculating the creation probability given by Eq. (31) for every successful creation, where the new $(n+1)$-configuration satisfies the applied cluster definition. In our simulations the density of the inserted molecules was 10 times the liquid density of argon. The decay probability is gained by calculating the annihilation probability given by Eq. (30) for every molecule in the cluster. Only annihilations, where the remaining $(n-1)$-cluster does not violate the applied cluster definition, are taken into account.

In this paper we have used the two methods for the simulations of vapor–liquid nucleation of argon. The interaction between the argon atoms is described by the Lennard–Jones potential

$$\varphi_{ij}(R_{ij}) = 4\varepsilon\left\{\left(\frac{\sigma}{R_{ij}}\right)^{12} - \left(\frac{\sigma}{R_{ij}}\right)^{6}\right\}, \tag{42}$$

where R_{ij} is the distance between molecules i and j, and ε and σ are the energy and distance parameters of the selected potential, respectively. In our simulations we used the full potential with parameters $\varepsilon = 119.4\,\mathrm{K}$ and $\sigma = 3.4\,\text{Å}$. We used no cutoff. In some simulations we used a hard sphere of radius ranging from 2 to 3 Å around each molecule in the cluster. This was taken into account when calculating v_{free}.

We applied the Stillinger cluster definition for both methods, stating that each molecule in a cluster must have another cluster molecule within some given connectivity distance, and that no molecules that do not belong to the cluster can within the connectivity distance. Here, we have taken the connectivity distance to be 1.5σ, which is the standard connectivity distance for Lennard–Jones particles describing the first minimum in the radial distribution function of the liquid.

In the simulations we equilibrated the randomly generated initial cluster configurations containing n argon atoms for $2n\times10^5$ Monte Carlo steps in both methods. Then, for the free energy calculation we generated another $n\times10^6$ configurations. In the overlapping distribution simulation the potential energy difference histograms were generated from all the sampled configurations. In the growth/decay simulation the growth and decay probabilities were calculated for every 100th configuration.

6. Results and discussion

Using the two methods described in the earlier sections we calculated the work of formation at different saturation ratios and temperatures. We used the experimental values of saturated vapor pressures as the reference value for the monomer density in saturated vapor (Lide, 2002). The size of the clusters ranged from two to two hundred molecules. We will first take a look at the effect of the factor λ and the δ-term introduced in Section 2. Later we compare the results given by the two methods. We will also make a comparison with earlier studies.

Factor λ can be used to give the non-interacting molecule in system B a slight interaction, which prevents it overlapping with another molecule. Our simulations show that the choice of λ, when simulating

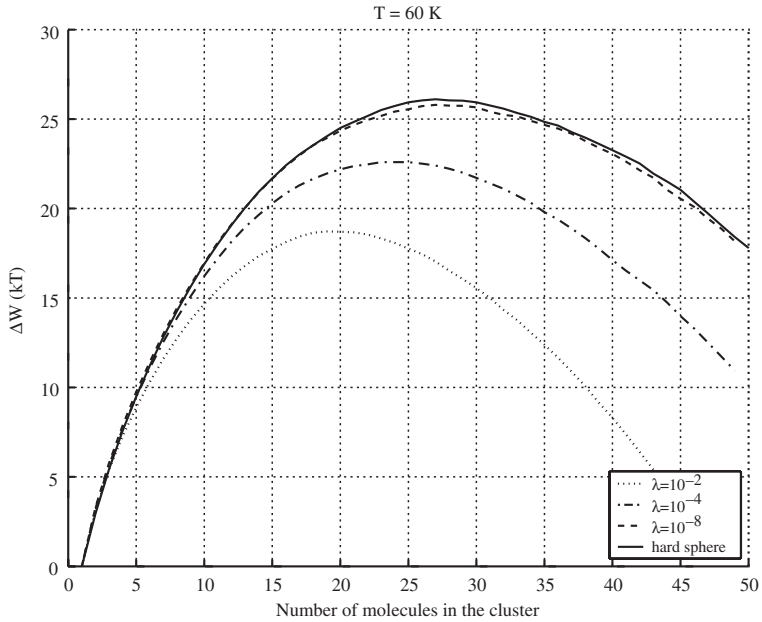

Fig. 4. The effect of the variation of the factor λ on the work of formation. $T=60$ K, $S=50$. The curves correspond to values $\lambda=10^{-2}$, $\lambda=10^{-4}$, and $\lambda=10^{-8}$. The reference curve corresponds to $\lambda=0$, when there is a hard sphere at 2.822 Å around the cluster molecules.

system B, plays a very important role in the simulation results. For the cluster definition we have used there is a dramatical difference between the results obtained by $\lambda=0.01$ and $\lambda=10^{-8}$, as can be seen in Fig. 4. In contrast, prevention of the overlap by a hard sphere radius works well. In our simulations all the nearest allowed distances between 2 Å and 3 Å yielded the same result, when the value of λ was set to 0. Our final selection for the limiting distance was 0.83σ, which corresponds to 2.822 Å.

The δ-term accounts for the fact that turning the interaction of one molecule off might result in the remaining molecules to form two separate clusters instead of one cluster. We have shown in Section 2 that,

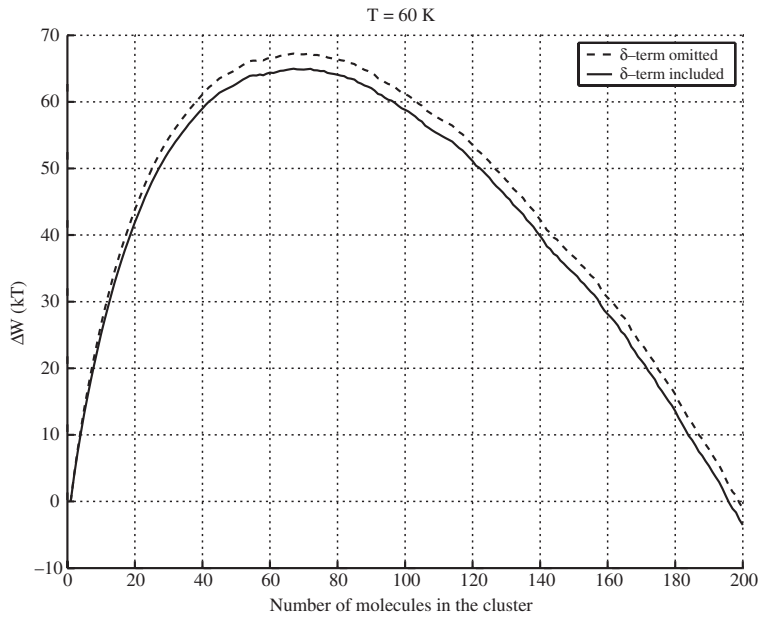

Fig. 5. The effect of the δ-term on the work of formation at $T=60$ K, $S=20$.

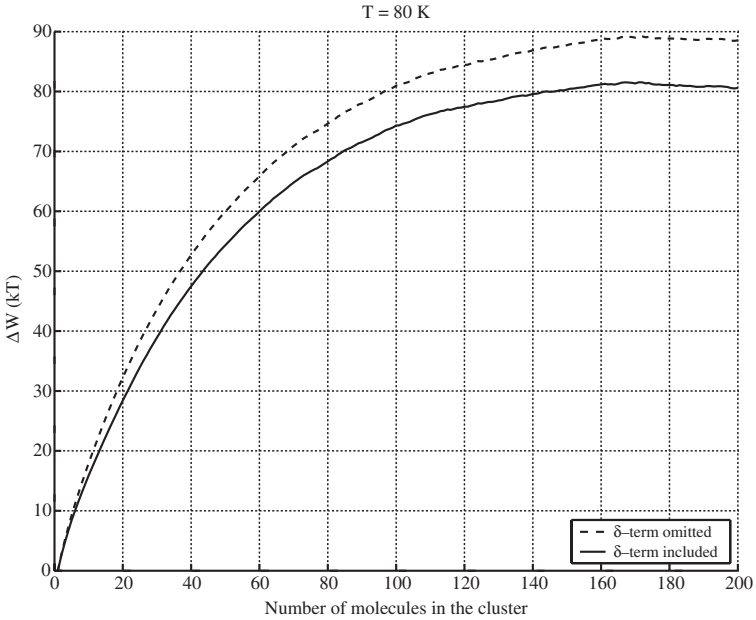

Fig. 6. The effect of the δ-term on the work of formation at $T=80\,K$, $S=3$.

when applying the discrete summation method in the calculation of the reversible work of formation, it is necessary to take into account the fact that the configurational space is larger for an n-cluster than for the system containing $(n-1)$-cluster plus one free molecule. If we do so, an additional term to the original formulas (Hale and Ward, 1982; Hale, 1996) arises. Figs. 5 and 6 show the work of formation both the δ-term omitted and included in 60 and 80 K, respectively. As seen in the figures, it can be significant for the Stillinger cluster definition. At 60 K the magnitude of the effect is approximately $3kT$, but the effect gets

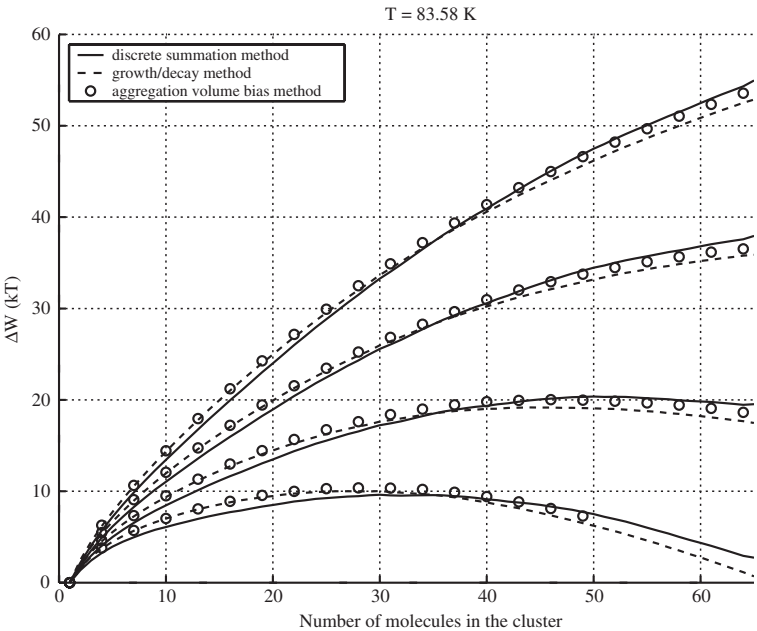

Fig. 7. Comparison between the work of formation results obtained by the methods we have used and Chen et al. (2001). Starting from the top, the curve triplets correspond to the following monomer concentrations in the surrounding vapor: $5.75\times10^{-3}/\sigma^3$, $7.5\times10^{-3}/\sigma^3$, $10^{-2}/\sigma^3$, and $1.3\times10^{-2}/\sigma^3$. $T*=0.7$ ($T=83.58\,K$).

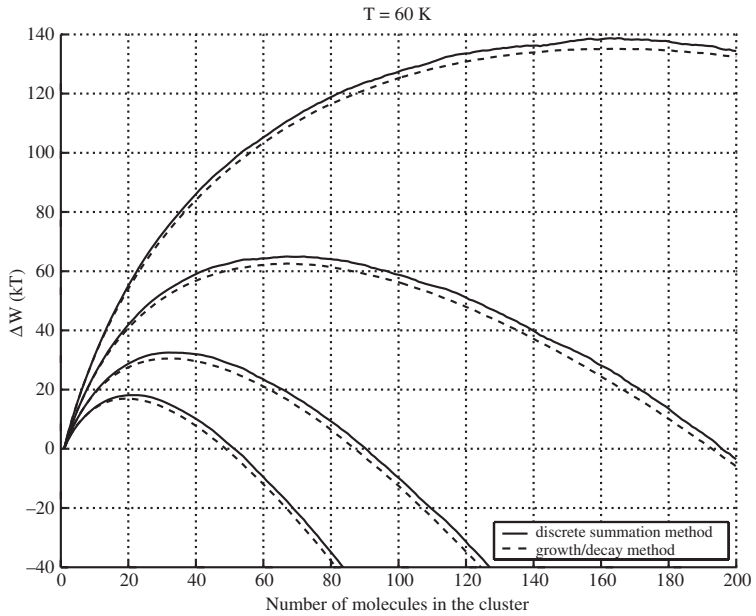

Fig. 8. The work of formation curves obtained by the two methods used in this study. The solid lines correspond to the values obtained using the discrete summation method, and the dashed lines show the results of the growth/decay method. Starting from the top, the curve pairs correspond to saturation ratios 10, 20, 40, and 70. T=60 K.

stronger at higher temperatures being already approximately $10kT$ at 80 K. This follows from the fact that at higher temperatures the cluster configurations are looser, making it more probable to have clusters split in two parts, which are interconnected only by the non-interacting molecule.

We can estimate the importance of the difference for the cluster definition by Lee, Barker and Abraham

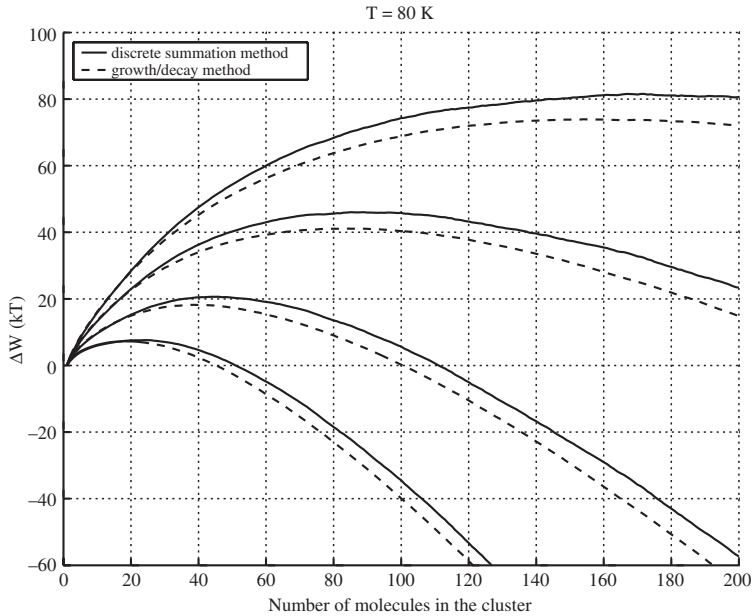

Fig. 9. The work of formation curves obtained by the two methods used in this study. The solid lines correspond to the values obtained using the discrete summation method, and the dashed lines show the results of the growth/decay method. Starting from the top, the curve pairs correspond to saturation ratios 3, 4, 6, and 9. T=80 K.

(LBA) (Lee et al., 1973) or a similar definition by Hale (1996). According to the LBA cluster definition n molecules form a cluster, when they can be confined with a sphere of a certain volume v_n. The center of the sphere is assumed to be in the center of mass of these n molecules. The volume of the sphere is chosen according to some physical criteria leading to the volume being usually proportional to n. The results of our formalism concerning the boundary condition set by the cluster definition are shown in Eqs. (20), (21), and (29). When applying our formalism to clusters defined by the LBA or Hale definitions, the ratio of the configurational integrals for the n-cluster and for the system containing $(n-1)$-cluster plus one free molecule cannot exceed the ratio of the configurational spaces v_n/v_{n-1}, i.e. $n/(n-1)$. Hence, the additional term cannot be more than

$$\text{difference} = -kT\sum_{i=2}^{n}[1+\delta(i)] = -kT\sum_{i=2}^{n}\ln\frac{i}{i-1} = -kT\ln n. \quad (43)$$

Comparing the latter expression with the data in Figs. 5 and 6 we conclude that for the LBA type of cluster definitions the additional term seems to be of less significance than for the Stillinger cluster definition.

Fig. 7 shows the results from the two methods discussed in this paper compared with the results from the "aggregation volume bias method" developed by Chen et al. (2001). The results from all the three methods agree within the calculation accuracy.

The calculations of the free energy barriers up to cluster sizes containing 200 argon atoms were carried out with the two methods at 60 K and 80 K temperatures. The same number of configurations was sampled in these calculations in both methods.

From the results shown in Figs. 8 and 9 we can see that the two methods produce comparatively similar results. However, there is some deviation, especially at $T=80$ K. The differences between the work of formation of n- and $(n-1)$-clusters $\delta W_{n,n-1}$ are shown in Figs. 10 and 11. At both temperatures the overlapping distribution method gives higher values for the difference in a certain size region. At $T=60$ K the region covers cluster sizes 10–30, and at $T=80$ K this region stretches from 15-molecule clusters up to 60-molecule clusters.

The differences shown in Figs. 10 and 11 also show that the growth/decay method gives more accurate results, when the number of sampled configurations is equivalent. However, this does not directly tell anything about the difference between the computational efficiencies between the two methods, as the configurations are sampled around ten times faster with the discrete summation method. The growth/decay method requires additional computational time for the grand canonical creation and annihilation Monte Carlo moves. From additional runs we could see that the growth/decay achieves the same

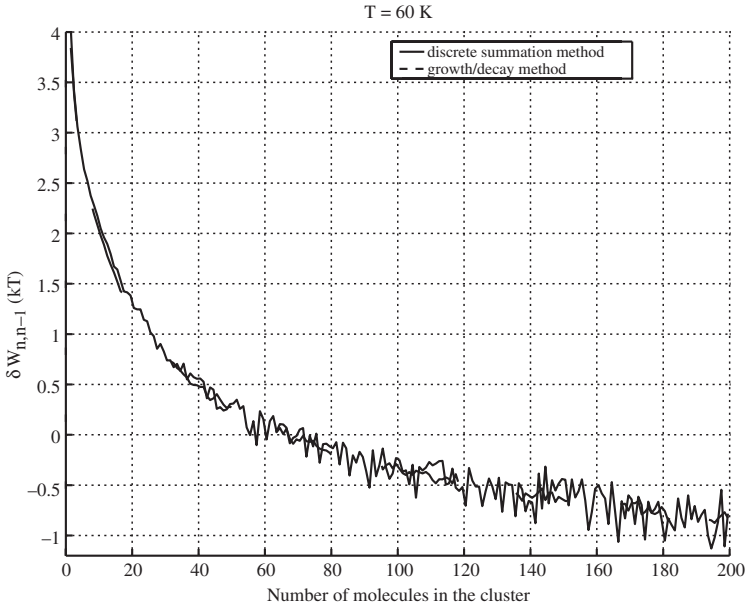

Fig. 10. The difference of the work of formation between an n-cluster and an $(n-1)$-cluster $\delta W_{n,n-1}$ at 60 K. The solid line corresponds to the values obtained using the discrete summation method, and the dashed line shows the results of the growth/decay method. $S=20$.

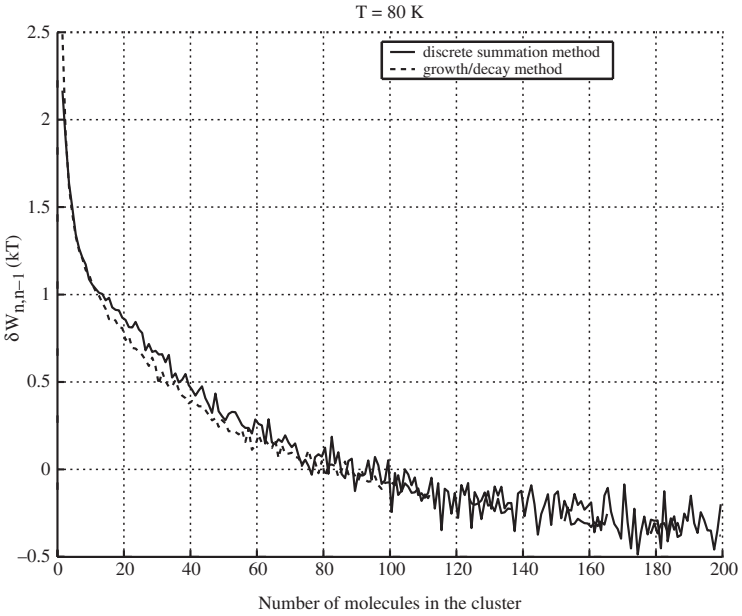

Fig. 11. The difference of the work of formation between an n-cluster and an $(n-1)$-cluster $\delta W_{n,n-1}$ at 80 K. The solid line corresponds to the values obtained using the discrete summation method, and the dashed line shows the results of the growth/decay method. $S=4$.

computational accuracy for the free energy calculation with around one-tenth of the sampled configurations, making the methods equivalent in efficiency.

7. Conclusions

In this paper we have compared two molecular Monte Carlo simulation methods, which are both capable of calculating the free energy of cluster formation by simulating single isolated clusters without the surrounding vapor. The comparison was made by calculating the free energy barriers for Lennard–Jones argon nucleation at temperatures 60 K and 80 K for several fictitious surrounding vapor densities. Both methods give essentially equivalent results as the methods where the vapor phase is explicitly included. The advantage of these methods is that the simulated system is only the size of the cluster. This makes them computationally efficient. The efficiency of the two methods is nearly equivalent. The given number of configurations is sampled around ten times faster with the discrete summation method than with the growth/decay method, but the growth/decay method gives the same accuracy for the free energy calculation with around one-tenth of the analysed configurations than the discrete summation method. In this paper we have used the same amount of configurations in the calculations, making the results gained from the growth/decay method more accurate.

We have not included the vapor–cluster interaction and the excluded volume terms for the calculation of free energy barriers. Whereas this interaction is negligible for low densities of the gas phase, it has been shown that for high densities of the nucleating vapor the vapor–cluster interaction has a significant effect on the results, but these terms could be easily added separately to results, as Oh and Zeng (1999) have shown. The cluster–vapor interaction would then be approximated with a mean field interaction.

Our results for the work of formation differ from the results based on the formalism of Hale and Ward (1982) by a term, which arises from the nonequivalence of the configurational space between the ensemble A, which contains n interacting molecules, and the ensemble B, which contains $n-1$ interacting molecules plus one free molecule. At $T=80$ K the order of the term is around $10kT$ for the work of formation of the critical cluster. When the additional term is included in the free energy calculations, the discrete summation method and the growth/decay method give nearly identical results.

Furthermore, we have shown that the free molecule cannot be represented with an arbitrarily small interaction term, which would prevent molecular overlapping in system B. The results show a strong dependence on the size of the interaction even for very small values. Instead, the molecular overlapping should be prevented by a hard sphere around each cluster molecule. An

interval where the results are independent of the size of the sphere for a wide range of values can be found.

References

Abraham, F.F., 1974. Homogenous nucleation theory. Advances in Theoretical Chemistry. Academic Press, New York.

Band, W., 1939a. Dissociation treatment of condensing systems. J. Chem. Phys. 7, 324–326.

Band, W., 1939b. Dissociation treatment of condensing systems: II. J. Chem. Phys. 7, 927–931.

Becker, R., Döring, W., 1935. Kinetische Behandlung der Keimbildung in übersättigten Dämpfen. Ann. Phys. (Leipz.) 24, 719–752.

Bennett, C.H., 1976. Efficient estimation of free energy differences from Monte Carlo data. J. Comput. Phys. 22, 245–268.

Bijl, A., 1938. Discontinuities in the energy and specific heat. PhD thesis, University of Leiden, Leiden, Germany.

Chen, B., Siepmann, J.I., Oh, K.J., Klein, M.L., 2001. Aggregation-volume-bias Monte Carlo simulations of vapor–liquid nucleation barriers for Lennard–Jonesium. J. Chem. Phys. 115, 10903–10913.

Dillmann, A., Meier, G.E.A., 1991. A refined droplet approach to the problem of homogeneous nucleation from the vapor phase. J Chem. Phys. 94, 3872–3884.

Frenkel, J., 1939a. A general theory of heterophase fluctuations and pre-transition phenomena. J. Chem. Phys. 7, 538–547.

Frenkel, J., 1939b. Statistical theory of condensation phenomena. J. Chem. Phys. 7, 200–201.

Garcia, N.G., Soler Torroja, J.M., 1981. Monte Carlo calculation of argon clusters in homogeneous nucleation. Phys. Rev. Lett. 47, 186–190.

Hale, B.N., 1996. Monte Carlo calculations of effective surface tension for small clusters. Aust. J. Phys. 49, 425–434.

Hale, B.N., Ward, R., 1982. A Monte Carlo method for approximating critical cluster size in the nucleation of model systems. J. Stat. Phys. 28, 487–495.

Hoare, M.R., Pal, P., Wegener, P.P., 1980. Argon clusters and homogeneous nucleation: comparison of experiment and theory. J. Colloid Interface Sci. 75, 126–137.

Kashchiev, D., 2000. Nucleation: Basic Theory with Applications. Butterworth-Heinemann, Oxford.

Kulmala, M., 2003. How particles nucleate and grow. Science 302, 1000–1001.

Kusaka, I., Wang, Z.G., Seinfeld, J.H., 1998. Direct evaluation of the equilibrium distribution of physical clusters by a grand canonical Monte Carlo simulation. J. Chem. Phys. 108, 3416–3423.

Lee, J.K., Barker, J.A., Abraham, F.F., 1973. Theory and Monte Carlo simulations of physical clusters in the imperfect vapor. J. Chem. Phys. 58, 3166–3180.

Lewis, J.W., Williams, W.D., 1974. AEDCTR32. Technical report, National Technical Information Service No. AD782445.

Lide, D.R. (Ed.), 2002. CRC Handbook of Chemistry and Physics, 83rd edition. CRC Press, Boca Raton.

Lothe, J., Pound, G.M., 1962. Reconsiderations of nucleation theory. J. Chem. Phys. 36, 2080–2085.

Matthew, M.W., Steinwandel, J., 1983. An experimental study of argon condensation in cryogenic shock tubes. J. Aerosol Sci. 14, 755–763.

Merikanto, J., Vehkamäki, H., Zapadinsky, E., 2004. Monte Carlo simulations of critical cluster sizes and nucleation rates of water. J. Chem. Phys. 121, 914–924.

Oh, K., Zeng, X., 1999. Formation free energy of clusters in vapour–liquid nucleation: a Monte Carlo simulation study. J. Chem. Phys. 110, 4471–4476.

Oh, K.J., Zeng, X.C., 2000. A small-system ensemble Monte Carlo simulation of supersaturated vapor: evaluation of barrier to nucleation. J. Chem. Phys. 112, 294–300.

Oxtoby, D.W., Evans, R., 1988. Nonclassical nucleation theory for the gas–liquid transition. J. Chem. Phys. 89, 7521–7530.

Pierce, T., Sherman, P.M., McBride, D.D., 1971. Condensation of argon in a supersonic stream. Astronaut. Acta 16, 1–4.

Reiss, H., Bowles, R.K., 1999. Some fundamental statistical mechanical relations concerning physical clusters of interest to nucleation theory. J. Chem. Phys. 111, 7501–7504.

Stein, G.D., 1974. Report to office of naval research. Technical report, National Technical Information Service. No. ADA007357/7GI.

Steinwandel, J., Buchholz, T., 1984. Homogeneous condensation of argon: an experimental study using the nozzle flow of a cryogenic Ludwieg tube. Aerosol Sci. Tech. 3, 71–76.

Stillinger, F.H., 1963. Rigorous basis of the Frenkel–Band theory of association equilibrium. J. Chem. Phys. 38, 1486–1494.

ten Wolde, P.R., Frenkel, D., 1998. Computer simulation study of gas–liquid nucleation in a Lennard–Jones system. J. Chem. Phys. 109, 9901–9918.

ten Wolde, P.R., Ruiz-Montero, M.J., Frenkel, D., 1999. Numerical calculation of the rate of homogeneous gas–liquid nucleation in a Lennard–Jones system. J. Chem. Phys. 110, 1591–1599.

Vehkamäki, H., Ford, I.J., 2000. Critical cluster size and droplet nucleation rate from growth and decay simulations of Lennard–Jones clusters. J. Chem. Phys. 112, 4193–4202.

Vehkamäki, H., Napari, I., Kulmala, M., Noppel, M., 2004. Stable ammonium bisulphate clusters in the atmosphere. Phys. Rev. Lett. 93, 148501.

Volmer, M., Weber, A., 1925. Keimbildung in übersättigten Gebilden. Z. Phys. Chem. 119, 277–301.

Wölk, J., Strey, R., 2001. Homogeneous nucleation of H_2O and D_2O in comparison: the isotope effect. J. Phys. Chem., B 105, 11683–11701.

Wu, B.J.C., Wegener, P.P., Stein, G.D., 1978. Homogeneous nucleation of argon carried in helium in supersonic nozzle flow. J. Chem. Phys. 69, 1776–1777.

Zahoransky, R.A., Höschele, J., Steinwandel, J., 1999. Homogeneous nucleation of argon in an unsteady hypersonic flow field. J. Chem. Phys. 110, 8842–8843.

Zeldovich, J., 1942. Theory of the formation of a new phase, cavitation. Zh. Eksp. Theor. Fiz. 12, 525–538.